



# Conversion of CO<sub>2</sub> to CH<sub>4</sub> by a Pulsed Hydrogen Plasma Shower Method

Keisuke Arita<sup>1</sup> and Satoru Iizuka<sup>1\*</sup>

<sup>1</sup>Department of Electrical Engineering, Graduate School of Engineering, Tohoku University, Aoba 6-6-05, Aramaki, Aoba-ku, Sendai 980-8579, Japan.

## Authors' contributions

The experiments were performed in collaboration with both authors. The data were analyzed by author KA under discussions with author SI. Both authors were approved the final manuscript.

## Article Information

DOI: 10.9734/BJAST/2016/26169

### Editor(s):

(1) Wen Shyang Chow, School of Materials and Mineral Resources Engineering, Engineering Campus, Universiti Sains Malaysia, Malaysia.

### Reviewers:

(1) Alexandre Gonçalves Pinheiro, Ceará State University, Brazil.

(2) Gamal G. Elaragi, Egyptian Atomic Energy, Egypt.

Complete Peer review History: <http://sciencedomain.org/review-history/14425>

Original Research Article

Received 4<sup>th</sup> April 2016  
Accepted 25<sup>th</sup> April 2016  
Published 3<sup>rd</sup> May 2016

## ABSTRACT

**Aims:** To suppress the emission of CO<sub>2</sub> to the environment and to save the consumption of fossil fuels, CO<sub>2</sub> was converted to CH<sub>4</sub> by a newly developed hydrogen shower method with a hydrogen pulse plasma.

**Study Design:** Research study.

**Place and Duration of Study:** This study was performed for 2013 - 2015 at Department of Electrical Engineering, Tohoku University, Sendai, Miyagi, Japan.

**Methodology:** The experiment was carried out in a small chamber which was divided into two parts by an orifice disc of 3-mm-thickness stainless plate with one 0.5-mm-diameter hole at the center. Hydrogen gas was supplied from the left part, where hydrogen radicals of H\* and H<sub>2</sub>\* were produced by a pulse discharge. Hydrogen radicals were supplied through the orifice from the left part to the right part as a hydrogen radical shower. Carbon dioxide was directly supplied to the right reaction part, where CO<sub>2</sub> was able to collide with hydrogen radicals and as a result CH<sub>4</sub> was produced.

**Results:** Dependences of CO<sub>2</sub> decomposition ratio  $\alpha$ , methane selectivity  $\beta$ , and energy efficiency  $\gamma$  on hydrogen flow rate, electrode distance, discharge tube diameter, applied voltage, electrode diameter, and gas feeding type were investigated. Methane was produced from carbon dioxide by

\*Corresponding author: E-mail: [iizuka@ecei.tohoku.ac.jp](mailto:iizuka@ecei.tohoku.ac.jp);

using a hydrogen radical shower method. Methane was only organic species produced from CO<sub>2</sub>. Only CO was detected as non-organic by-product. It was found that the decomposition ratio  $\alpha$ , methane selectivity  $\beta$ , and energy efficiency  $\gamma$  were  $\alpha = 32\%$ ,  $\beta = 37\%$ , and  $\gamma = 1.6$  L/kWh, respectively, under optimized condition at the flow rate ratio of CO<sub>2</sub>: H<sub>2</sub> = 1:2, gap distance of  $d = 6$  mm, and input power of  $P_{in} = 4.6$  W (1.2 kV, 3.8 mA) with a use of 6-mm-diameter electrode.

**Conclusion:** Energy efficiency in our case was fairly improved. Hydrogen radical shower method was very effective for the conversion of CO<sub>2</sub> to CH<sub>4</sub>.

*Keywords: Carbon dioxide; methane; hydrogen radical shower; pulse discharge.*

## 1. INTRODUCTION

Carbon dioxide CO<sub>2</sub> is one of the man-made greenhouse gases that are emitted by combustion of fossil fuels, such as coal, oil, and natural gas. Carbon dioxide is emitted from many power plants for generating electricity, power vehicles, heat homes, cook food and much more. However, fossil fuels are essentially a non-renewable energy source. Within the next 100 years it is widely believed that the cost of finding and extracting new underground resources will be much more expensive for everyday use. It might be also serious that CO<sub>2</sub> would cause global warming by absorbing and emitting radiation within the infrared range.

Therefore, the suppression of emission of carbon dioxide into the environment and the reduction of consumption of fossil fuels are crucial subject that must be settled urgently.

In order to suppress the emission of CO<sub>2</sub> into the environment from electrical power plants, for example, it might be desirable that CO<sub>2</sub> is collected before exhausting to convert it to methane, if any surplus electric power exists. This means that surplus electric energy can be converted to chemical bonding energy of methane. That is, the surplus electric energy can be stored as methane [1]. This method is superior to batteries, because the electric energy stored in batteries will be gradually lost by a natural discharge. On the contrary, the energy stored in methane will be conserved without any loss for many years.

In order to reduce CO<sub>2</sub> with hydrogen various experiments were carried out by using discharge system [2-9]. In most cases, CO<sub>2</sub> was reduced by CH<sub>4</sub> to form syngas of CO and H<sub>2</sub>, because methane is also one of the greenhouse gases [10-16]. Eliasson et al. [2] investigated the production of CH<sub>4</sub> by a dielectric barrier discharge with H<sub>2</sub> in detail. Mixed gas of CO<sub>2</sub> and H<sub>2</sub> was employed for CH<sub>4</sub> production. However,

for an efficient formation of methane a new innovative method has been expected.

The purpose of this study is to investigate fundamental process of the reduction of carbon dioxide by hydrogen radicals that were produced in H<sub>2</sub> discharge. Hydrogen radical shower was supplied to the plasma-free downstream reaction space where CO<sub>2</sub> was supplied. Since CH<sub>4</sub> production region was separated spatially from H<sub>2</sub> discharge region, a preferable conversion rate was expected, because deformation of CH<sub>4</sub> was able to be avoided in the plasma-free reaction space. Our method proposed here is quite unique to generate beneficial and reusable organic materials like methane by using low-pressure hydrogen discharges [17-19].

## 2. EXPERIMENTAL DETAILS

Schematic of the experimental apparatus is shown in Fig. 1. The chamber was divided into two parts by an orifice disc of 3-mm-thickness stainless plate with one 0.5-mm-diameter hole at the center. The left part was a hydrogen plasma source for the hydrogen radical production, consisting of a glass tube of 4 mm in inner diameter. Hydrogen gas was supplied from the left side into the plasma source region. The right part was a narrow reaction space consisting of a glass tube of 10 mm in inner diameter, terminated by double glass tubes, consisting of an inner glass tube of 4 mm in outer diameter and 2 mm in inner diameter, and an outer glass tube of 10 mm in outer diameter and 8 mm in inner diameter. Axial length of the reaction space between the orifice plate and the end of the double tube can be varied from 3 mm to 10 mm. Usually, it was set at 5 mm. There was no discharge in the reaction space. Carbon dioxide was fed directly into the reaction space through an inner tube of the double glass tubes from the right side. A stainless rod electrode of 1 mm in diameter was inserted into the glass tube from the left side. Hydrogen plasma was produced between the tip of the electrode and the metal

orifice plate grounded electrically. Here, hydrogen radicals of  $H^*$  and  $H_2^*$  were produced through the following reactions.



These radicals were injected into the reaction space through the orifice hole as a hydrogen radical shower. In this way,  $CO_2$  was able to collide with  $H^*$  and  $H_2^*$  radicals in the reaction space and as a result  $CH_4$  was produced. The gas produced was evacuated by a rotary pump through a circumferential gap between the outer and inner tubes of the double glass tube. Gas flow directions are indicated by arrows in Fig. 1.

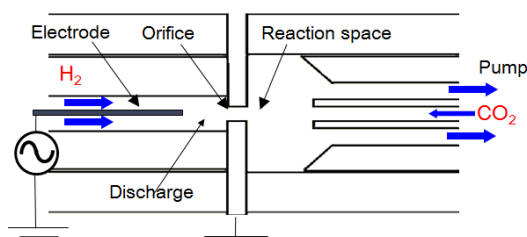


**Fig. 1. Schematic of the experimental setup**

The gas flow rate ratio of carbon dioxide to hydrogen and the total gas flow rate were controlled by mass flow controllers, independently. Total pressure was fixed at 200 Pa. Here, we employed a negative square-pulse voltage that was supplied to a small electrode. Pulse duration was fixed at 5  $\mu s$ . Repetition frequency of the square pulse was also fixed at 7.8 kHz. The gas after passing through the discharge region was sampled and analyzed by Fourier transform infrared spectroscopy (FTIR) by comparing the gas species before and after the discharge [17-19].

### 3. RESULTS

The results were evaluated by the following quantities.

(i)  $CO_2$  decomposition ratio  $\alpha$ :

$$\alpha = 1 - [CO_2]_1 / [CO_2]_0 \quad (3)$$

(ii)  $CH_4$  selectivity  $\beta$ :

$$\beta = [CH_4] / [\text{all carbon species produced}] \quad (4)$$

(iii) Energy efficiency  $\gamma$  (L/kWh) for  $CH_4$  production:

$$\gamma = [CH_4 \text{ produced in litter}] / (\text{electric energy consumed by the discharge}) \quad (5)$$

Here,  $[x]$  denotes amount of  $x$ , and suffix 0 and 1 correspond to the values before and after the discharge, respectively. These quantities show how much carbon in  $CO_2$  has been converted to methane.  $\gamma$  is an important factor to realize a suitable commercial system for producing methane in high efficiency. Using  $\alpha$  and  $\beta$ ,  $\gamma$  can be expressed as follows.

$$\gamma = \alpha\beta\Gamma / (\text{electric power for the discharge (W)}) \times 60 \quad (6)$$

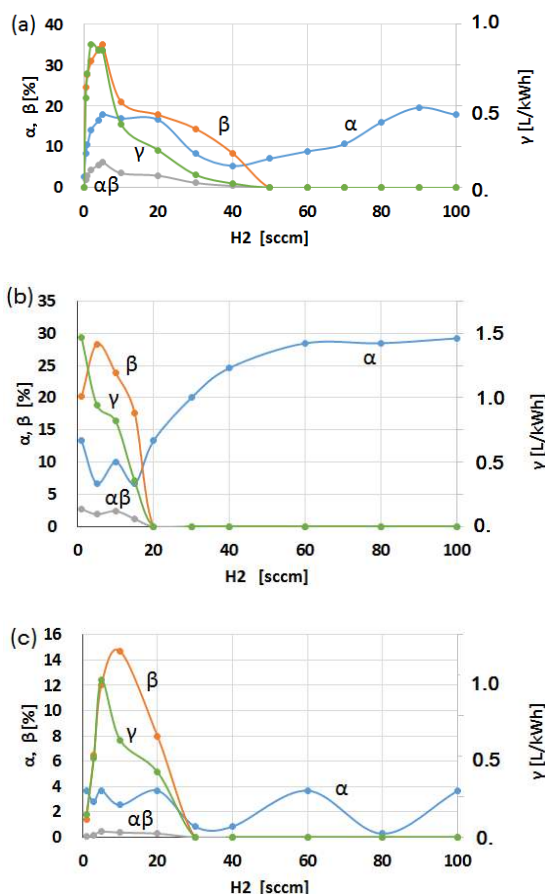
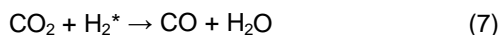


**Fig. 2. Variations of  $\alpha$ ,  $\beta$ ,  $\alpha\beta$ ,  $\gamma$  as a function of  $H_2$  flow rate in cases of  $CO_2 =$  (a) 1 sccm, (b) 5 sccm, and (c) 20 sccm in a 4-mm-diameter glass tube. Electrode distance is  $d = 2$  mm**

Here,  $\Gamma$  is initial gas flow rate of  $CO_2$  [scc/min; standard cubic centimeter per minute]. The change of gas species measured by FTIR showed that main carbon products were  $CH_4$  and  $CO$  through the whole experiment. Here,  $CO$  might come from the following dissociation reaction by hydrogen radicals in the reaction space.



Hydrocarbon species was only  $\text{CH}_4$ , and the other species like  $\text{HCOH}$  and  $\text{CH}_3\text{OH}$  were not detected and/or were negligibly small. We could not detect other  $\text{C}_2$  organic materials such as ethane, ethylene, and acetylene. But, the production of steam  $\text{H}_2\text{O}$  was detected. Therefore, it was shown that methane was only a hydrocarbon produced from  $\text{CO}_2$  in this system. Therefore, in this case, the reaction was rather simple and the methane selectivity  $\beta$  could be simply expressed by  $\beta = [\text{CH}_4] / ([\text{CH}_4] + [\text{CO}])$ .

### 3.1 $\text{H}_2$ Flow Rate Dependence

First, dependences of  $\text{CO}_2$  decomposition ratio  $\alpha$ , methane selectivity  $\beta$ , product  $\alpha\beta$ , and energy efficiency  $\gamma$  on hydrogen flow rate were shown in Fig. 2 with  $\text{CO}_2$  flow rate as a parameter. Here, electrode diameter was 1 mm, electrode distance was  $d = 2$  mm and the applied voltage was 1.25 kV under the total pressure of 200 Pa. The discharge took place in a glass tube of 4 mm in inner diameter.

When  $\text{CO}_2$  flow rate is 1 sccm,  $\alpha$  increases with  $\text{H}_2$  flow rate and attained to a broad maximum of 17 – 18% in the range of  $\text{H}_2 = 5 - 20$  sccm. Then,  $\alpha$  decreases with  $\text{H}_2$  and eventually increased again to about 20% as shown in Fig. 2(a). The variation of  $\beta$  was similar to that of  $\alpha$  in the range  $\text{H}_2 < 5$  sccm. However,  $\beta$  was simply decreased to zero in the range of  $\text{H}_2 = 10 - 50$  sccm. No methane was produced in the range  $\text{H}_2 > 50$  sccm. The maximum of  $\beta$  was about 35% in this case. Then, the maximum of the product  $\alpha\beta$  was about 6.3% at  $\text{H}_2 = 5$  sccm. That is, 6.3% of  $\text{CO}_2$  was converted to  $\text{CH}_4$ . The energy efficiency for methane production was also varied like  $\alpha\beta$  and its maximum attained was 0.9 L/kWh at  $\text{H}_2 = 5$  sccm.

The properties described above were not much changed when  $\text{CO}_2$  flow rate was increased to 5 sccm and 20 sccm, as shown in Figs. 2(b) and (c), respectively. Methane production was observed in a limited range of  $\text{H}_2 < 20$  sccm and  $< 30$  sccm in the cases of  $\text{CO}_2 = 5$  sccm and 20 sccm, respectively. The maximum of  $\alpha$  in this range was 14% in the case of  $\text{CO}_2 = 5$  sccm, and 4% in the case of  $\text{CO}_2 = 20$  sccm. On the other hand, the maximum  $\beta$  was 28.5% in the case of  $\text{CO}_2 = 5$  sccm, and 14.8% in the case of  $\text{CO}_2 = 20$  sccm. These values were smaller than 35% in the case of  $\text{CO}_2 = 1$  sccm. The product  $\alpha\beta$  was also decreased with an increase of  $\text{CO}_2$  flow rate. We got maximum  $\alpha\beta = 2.5\%$  and 0.08% in

the cases of  $\text{CO}_2 = 5$  sccm and 20 sccm, respectively. The variation of energy efficiency  $\gamma$  was not so simple. We got  $\gamma$  of 1.0 – 1.5 L/kWh in the cases of  $\text{CO}_2 = 5 - 20$  sccm.

### 3.2 Electrode Distance Dependence

The discharge took place under the condition with applied voltage of 1.25 kV and total pressure of 200 Pa. Fig. 3 shows variations of  $\alpha$ ,  $\beta$ ,  $\alpha\beta$ , and  $\gamma$  as a function of the electrode distance  $d$ . Decomposition of 40% was obtained when the electrode distance  $d$  was 2-3 mm. However,  $\alpha$  was decreased with an increase of  $d$  ( $> 4$  mm). On the contrary,  $\text{CH}_4$  selectivity  $\beta$  was increased with an increase of  $d$  ( $> 4$  mm).

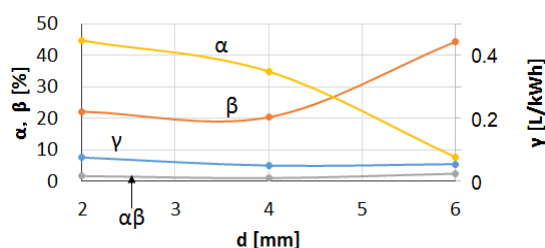


**Fig. 3. Variations of  $\alpha$ ,  $\beta$ ,  $\alpha\beta$ ,  $\gamma$  as a function of electrode distance  $d$  in case of  $\text{CO}_2/\text{H}_2 = 1$  sccm/10 sccm in a 4-mm-diameter glass tube**

When  $d$  was short, the density of hydrogen plasma increases by an increase of the strength of electric field between the electrode and the orifice. Then, such increase of hydrogen radical density might give rise to an enhancement of  $\text{CO}_2$  decomposition. On the contrary, with an increase in the electrode distance  $d$ ,  $\beta$  became relatively high. This might be due to that methane synthesis was proceeded with a relatively low density  $\text{H}_2^*$  radicals, where decomposition of  $\text{CO}_2$  by  $\text{H}_2^*$  collision was reduced. These different dependency of  $\alpha$  and  $\beta$  on  $d$  for  $d > 4$  mm was almost cancelled for  $d > 4$  mm, then the change of  $\alpha\beta$  was very small with an increase of  $d$ . Therefore, the energy efficiency  $\gamma$  was also not much changed by the electrode distance  $d$ .

### 3.3 Effect of Discharge Tube Diameter

As shown in Fig. 3, the methane selectivity  $\beta$  increased with the discharge length, although  $\text{CO}_2$  decomposition was decreased. In order to clarify the effect of the discharge volume on the methane production, the inner diameter of glass tube in the hydrogen discharge region was changed from 4 mm to 6 mm under the fixed discharge length at  $d = 6$  mm. Fig. 4 shows the

variations of  $\alpha$ ,  $\beta$ , and  $\gamma$  as a function of hydrogen flow rate. Here, the electrode diameter was 1 mm and  $\text{CO}_2$  flow rate was 1 sccm. As shown in Fig. 4,  $\text{CO}_2$  decomposition  $\alpha$  was 15% for  $\text{H}_2$  flow rate < 5 sccm, then  $\alpha$  was decreased to about 10% with an increase of  $\text{H}_2$ . Finally,  $\alpha$  became almost constant for  $\text{H}_2 > 10$  sccm. Methane selectivity  $\beta$  was increased with an increase of  $\text{H}_2$  flow rate, and attained to a maximum value of 54% when  $\text{H}_2 = 20$  sccm. Energy efficiency  $\gamma$  was also increased with  $\text{H}_2$  and attained to the maximum of 0.45 L/kWh at  $\text{H}_2 = 5$  sccm. By comparing these values with the results in Fig. 3 for the discharge with  $d = 6$  mm in the 4-mm-diameter tube, it was found that the discharge tube diameter was not so important for the improvement of the parameters  $\alpha$  and  $\beta$ . In both cases, we got  $\alpha \sim 9\%$  and  $\beta \sim 43\%$ .

### 3.4 Effect of Applied Voltage

Dependence of  $\alpha$ ,  $\beta$ ,  $\alpha\beta$ , and  $\gamma$  on the applied voltage is shown in Fig. 5. Here,  $\text{CO}_2$  flow rate was 1 sccm and  $\text{H}_2$  flow rate was 5 sccm. We got a large  $\beta$  when higher voltage was applied to the electrode. On the contrary,  $\alpha$  was decreased in the higher applied voltage regime. Eventually, the product  $\alpha\beta$  was saturated at around 10% for the applied voltage > 1.0 kV. On the other hand,  $\gamma$  became maximum with a decrease of the applied voltage. We got 1.4 L/kWh when the applied voltage was 1.0 kV.

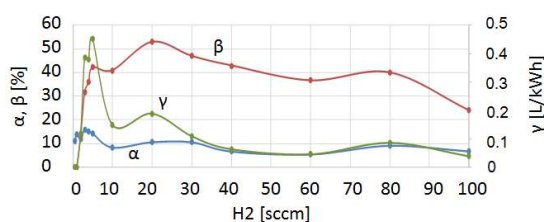


**Fig. 4. Variations of  $\alpha$ ,  $\beta$ , and  $\gamma$  as a function of  $\text{H}_2$  flow rate in case of  $\text{CO}_2$  sccm in a 6-mm-diameter glass tube. Electrode distance  $d = 6$  mm**

### 3.5 Effect of Electrode Diameter

Finally, the diameter of the electrode for the hydrogen discharge was changed in the 6-mm-diameter glass tube. Dependence of  $\alpha$ ,  $\beta$ , and  $\gamma$  on hydrogen flow rate is shown in Fig. 6(a), (b), and (c) for the electrode diameter of 1 mm, 3 mm, and 5 mm, respectively. We found that  $\alpha$ ,  $\beta$ , and  $\gamma$  were dependent on the diameter of the discharge

electrode. For a small diameter electrode methane selectivity  $\beta$  became large. The maximum of  $\beta$  was about 54% at  $\text{H}_2$  flow rate of 20 sccm. However,  $\beta$  was slightly decreased to 42% at  $\text{H}_2 = 5$  sccm. On the other hand, the maximum of  $\text{CO}_2$  decomposition rate  $\alpha$  was about 15% at  $\text{H}_2$  flow rate of 5 sccm as shown in Fig. 6(a).

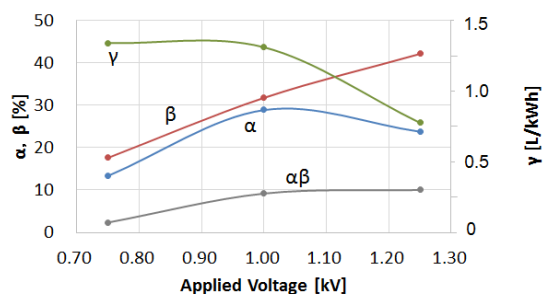


**Fig. 5. Variations of  $\alpha$ ,  $\beta$ ,  $\alpha\beta$ , and  $\gamma$  as a function of applied voltage in a 6-mm-diameter glass tube.  $\text{CO}_2/\text{H}_2 = 1$  sccm/5 sccm**

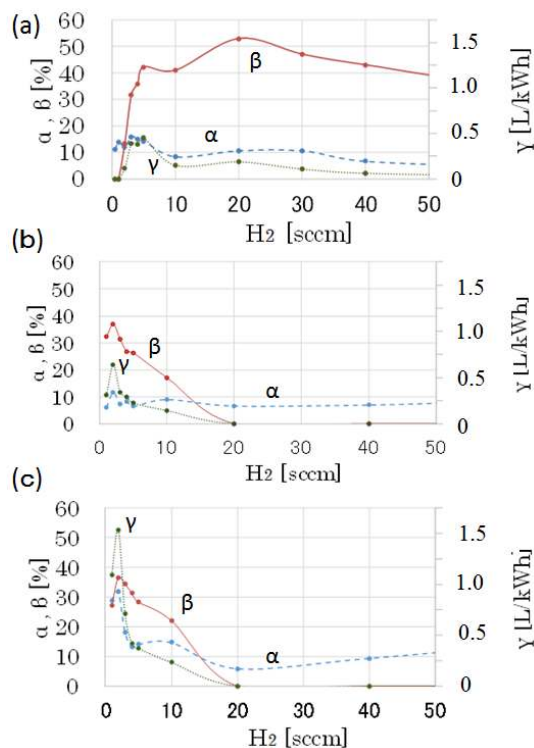


**Fig. 6. Variations of  $\alpha$ ,  $\beta$ , and  $\gamma$  as a function of hydrogen flow rate in three different cases of electrode diameters. (a) 1 mm, (b) 3 mm, and (c) 5 mm in a 6-mm-diameter glass tube. Applied voltage is 1.25 kV.  $\text{CO}_2 = 1$  sccm**

In the cases of the electrode diameter of 3 mm and 5 mm, the maximum of  $\alpha$  and  $\beta$  took place for a smaller  $H_2$  flow rate regime around  $H_2 = 2$  sccm. A big difference was observed in  $\alpha$  and  $\beta$  when the electrode diameter was 5 mm as shown in Fig. 6(c).  $\alpha$  was increased from 12% to 32% when the electrode diameter was increased from 3 mm to 5 mm, although  $\beta$  was not much changed. The maximum  $\beta$  attained to about 38% in both cases of 3 mm and 5 mm. When the electrode diameter was 5 mm, the energy efficiency  $\gamma$  attained to 1.6 L/kWh with  $\alpha = 32\%$  and  $\beta = 37\%$ , which was the most optimized condition in our experiment. It was also worthwhile noting that such optimum condition took place in a low hydrogen flow rate of 2 sccm. This was very important for saving hydrogen consumption for the production of methane.

### 3.6 Effect of Gas Feeding Style

As shown in Fig. 1, the gas feeding of  $H_2$  and  $CO_2$  is separated, i.e.,  $H_2$  was fed from the left side and  $CO_2$  was fed from the right side. In order to study the effect of gas feeding style,  $CO_2$  was mixed with  $H_2$  before feeding to the experimental apparatus, and the mixed gas was fed to the discharge region from the left side. In this case, the gas feeding from the right hand side was closed. The mixed gas was evacuated to the right side through a circumferential gap between the inner and outer glass tubes of the double glass tube. Fig. 7 shows  $H_2$  flow rate dependence of  $\alpha$ ,  $\beta$ , and  $\gamma$  for the cases of (a) separated gas feeding and (b) mixed gas feeding at  $CO_2$  flow rate of 1 sccm. The variations of  $\alpha$ ,  $\beta$ , and  $\gamma$  were drastically changed in the regime  $H_2 < 5$  sccm. In the separated case (a), both  $\alpha$  and  $\beta$  were increased and attained to the local maxima at  $H_2 \sim 1$  sccm, then these values decreased with  $H_2$  flow rate.  $\alpha$  and  $\beta$  were 9% and 28% at  $H_2 = 1$  sccm, respectively. In this case,  $\gamma$  also became the maximum of 0.5 L/kWh. On the other hand, in the case of the mixed gas feeding (b), no methane production was observed for  $H_2 < 3$  sccm. That is, at least 3 sccm of  $H_2$  was necessary for the  $CH_4$  production. We got that  $\alpha$  was 37%,  $\beta$  was 18%, and  $\gamma$  was 0.5 L/kWh at  $H_2 = 5$  sccm. That is, in the case of the separated gas feeding style, almost same energy efficiency  $\gamma$  was obtained by using a small amount of hydrogen consumption, i.e., 1/5  $H_2$  flow rate, compared to a mixed gas feeding style. It was found that the separated gas feeding style was quite effective for reducing  $H_2$  consumption for the generation of  $CH_4$ .

## 4. DISCUSSION

In our hydrogen radical shower method two processes are considered. One is a process for hydrogen radical production in the hydrogen plasma in the upper stream discharge space. The other is a process for  $CH_4$  production by a reaction of  $CO_2$  with hydrogen radicals in the downstream reaction space.

The production efficiency of hydrogen radicals was strongly dependent on the electron energy distribution function and electron density in the hydrogen plasma. It was found that the discharge length  $d$  gave an effect for  $CO_2$  decomposition and  $CH_4$  selectivity as shown in Fig. 3. When  $d$  was short, high energy tail electrons, accelerated by a large electric field between the electrodes, might excite and decompose  $H_2$ . And the reaction in Eqs. (1) and (2) were proceeded. Then,  $CO_2$  decomposition was enhanced together with  $CH_4$  production in the reaction space. On the other hand, when  $d$  was long, electron energy in the discharge space diminished, resulting in a decrease of  $CO_2$  decomposition and an increase of  $CH_4$  selectivity. However, it should be noted that an increase of the applied voltage did not simply result in an increase of  $CO_2$  decomposition as shown in Fig. 5. When the supplied power was increased, a power loss by heating the electrode tip was not negligible, which might cause a plasma density decrease and an eventual decrease of the energy efficiency  $\gamma$ .

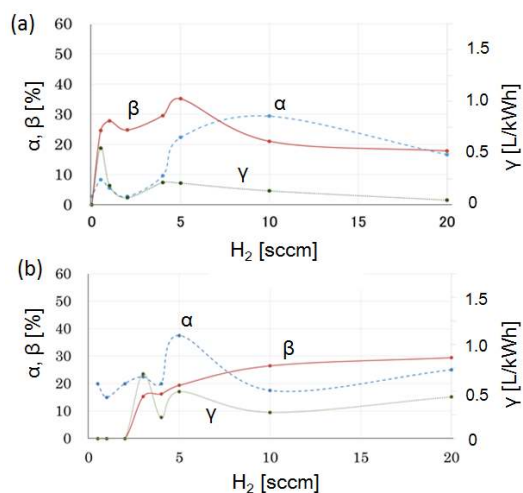


**Fig. 7. Variations of  $\alpha$ ,  $\beta$ , and  $\gamma$  as a function of hydrogen flow rate for (a) separated and (b) mixed gas feedings. Applied voltage is 1.25 kV.  $CO_2 = 1$  sccm**

Electrode diameter was found to be very important for the methane production. The optimum condition was obtained when CO<sub>2</sub>/H<sub>2</sub> flow rate was 1sccm/2 sccm, when the hydrogen plasma was produced with 5mm diameter electrode in a 6 mm diameter glass tube as shown in Fig. 6(c). We got that CO<sub>2</sub> decomposition ratio  $\alpha$  was 32% and the CH<sub>4</sub> selectivity  $\beta$  was 37%, where the product  $\alpha\beta$  attained to approximately 12%. The energy efficiency  $\gamma$  for the CH<sub>4</sub> production was 1.6 L/kWh. Flow rate ratio of CO<sub>2</sub>/H<sub>2</sub>=1/2 was quite preferable, because only small amount of hydrogen was required for CH<sub>4</sub> production. We can save the hydrogen consumption. This point was confirmed by introducing a mixed gas feeding discharge as shown in Fig. 7(b), where no methane was produced in the lower H<sub>2</sub> flow rate regime. The reason why the suitable gas mixing ratio of CO<sub>2</sub>/H<sub>2</sub> =1/2 was different from the stoichiometry ratio of 1/4, i.e., CO<sub>2</sub> + 4H<sub>2</sub> → CH<sub>4</sub> + H<sub>2</sub>O, might be due to an increase of H<sub>2</sub><sup>\*</sup>/H<sub>2</sub> ratio in the pure hydrogen plasma. The more H<sub>2</sub><sup>\*</sup> radicals were produced in the hydrogen discharge, the less input amount of H<sub>2</sub> was necessary for proceeding the reaction with CO<sub>2</sub>, i.e., CO<sub>2</sub> + H<sub>2</sub><sup>\*</sup> → CO<sup>\*</sup> + H<sub>2</sub>O.

The energy efficiency  $\gamma$  described above did not include the energy for generating H<sub>2</sub> from the water, for example. Electrolysis is a promising option for hydrogen production from renewable resources. Industrial electrolyzer have a nominal hydrogen production efficiency of around 70% [20,21]. As described above, in our experiment, CO<sub>2</sub> was decomposed to form CO<sup>\*</sup> by H<sub>2</sub><sup>\*</sup> and H<sup>\*</sup> radicals in the plasma-free reaction space. Then, CO<sup>\*</sup> was reduced further by H<sub>2</sub><sup>\*</sup> and H<sup>\*</sup>, and finally CH<sub>4</sub> was produced. This process was quite similar to Sabatier reaction, where CO<sub>2</sub> was dissociated to CO<sup>\*</sup> → C<sup>\*</sup> + O<sup>\*</sup> on a heated Ni surface at 200 – 400°C. Then, H<sub>2</sub> reacted with C<sup>\*</sup> and O<sup>\*</sup> on Ni surface to generate CH<sub>4</sub> [22,23]. In our case, the hydrogen radicals produced in hydrogen plasma played a similar role as a catalysis effect of Ni.

Finally, we discuss a carbon balance. As mentioned above, the materials containing carbon, produced by the discharge, were simply CH<sub>4</sub> and CO. Methanol was scarcely produced. The other carbon materials such as HCOH and C<sub>2</sub> hydrocarbons like ethane, ethylene, and acetylene were not detected. Visible carbon film deposition was not detected. This might be due to that the reaction among CH<sub>4</sub> for hydrocarbon

polymerization was restricted by the sufficient amount of hydrogen radicals injection into the downstream reaction space. Therefore, the carbon balance was simply expressed as  $\alpha[\text{CO}_2] \sim \alpha\beta[\text{CH}_4] + \alpha(1-\beta)[\text{CO}]$ .

It should be also noted that  $\gamma$  in our discharge system ( $\alpha = 32\%$ ,  $\beta = 37\%$ , and  $\gamma = 1.6$  L/kWh in Fig. 6(c)) was much higher than that of conventional discharges. The energy efficiency in the case of high-pressure dielectric-barrier discharge (DBD) was reported to be 0.06 L/kWh, where  $\alpha = 12.4\%$ ,  $\beta = 3.2\%$ , and total flow rate  $\Gamma = 500$  sccm (CO<sub>2</sub>: H<sub>2</sub> = 1:3) for the input power of 500 W [2]. For a low pressure microwave discharge,  $\gamma = 0.027$  L/kWh was reported with  $\alpha = 81\%$  and  $\beta = 1.2\%$  at input power of 3 kW [5]. Therefore, energy efficiency in our case was fairly improved.

## 5. CONCLUSION

Methane was produced from carbon dioxide by using a hydrogen radical shower method. Methane was only organic species produced from CO<sub>2</sub>. Only CO was detected as non-organic by-product. We found that the decomposition ratio  $\alpha$ , methane selectivity  $\beta$ , and energy efficiency  $\gamma$  were  $\alpha = 32\%$ ,  $\beta = 37\%$ , and  $\gamma = 1.6$  L/kWh, respectively, under optimized condition at flow rate ratio of CO<sub>2</sub> : H<sub>2</sub> = 1 : 2, gap distance of  $d = 6$  mm, and input power of  $P_{in} = 4.6$  W (1.2 kV, 3.8 mA) with a use of 6-mm-diameter electrode. Hydrogen radical shower method was a quite effective for the conversion of CO<sub>2</sub> to CH<sub>4</sub>.

## COMPETING INTERESTS

Authors have declared that no competing interests exist.

## REFERENCES

1. Struckmann LKR, Pesched A, Rauschenbach RH, Sundmacher K. Assessment of methanol synthesis utilizing exhaust CO<sub>2</sub> for chemical storage of electrical energy. *Ind. Eng. Chem. Res.* 2010;49:11073-11078.
2. Eliasson B, Kogelschatz U, Xue B, Zhou LM. Hydrogenation of carbon dioxide to methanol with a discharge-activated catalyst. *Ind. Eng. Chem. Res.* 1998;37:3350-3357.

3. Lunsford JH. Catalytic conversion of methane to more useful chemicals and fuels: A challenge for the 21st century. *Catal. Today*. 2000;63:165-174.
4. McDonough W, Braungart M, Anastas P, Zimmerman J. Peer reviewed: Applying the principles of green engineering to cradle-to-cradle design. *Environ. Sci. Technol.* 2003;37:434A-441A.
5. Gouyard V, Ttibouet J, Duperyrat CB. Influence of the plasma power supply nature on the plasma-catalyst synergism for the carbon dioxide reforming of methane. *IEEE Trans. Plasma Sci.* 2009;37:2342-2346.
6. Larkin DW, Lobban LL, Mallinson RG. Production of organic oxygenates in the partial oxidation of methane in a silent electric discharge reactor. *Ind. Eng. Chem. Res.* 2001;4:1594-1601.
7. Mei D, Zhu X, He YK, Yan JD, Tu X. Plasma-assisted conversion of CO<sub>2</sub> in a dielectric barrier discharge reactor: Understanding the effect of packing materials. *Plasma Sources Sci. Technol.* 2015;24:015011.
8. Hoeben WFLM, Boekhoven W, Beckers FJCM, Van Heesch EJM, Pemen AJM. Partial oxidation of methane by pulsed corona discharges. *J. Phys. D: Appl. Phys.* 2014;47:355202.
9. Zhu B, Li XS, Liu JL, Zhu X, Zhu AM. Kinetics study on carbon dioxide reforming of methane in kilohertz spark-discharge plasma. *Chem. Eng. J.* 2015;264:445-452.
10. Ross JRH. Natural gas reforming and CO<sub>2</sub> mitigation. *Catal. Today*. 2005;100:151-158.
11. Mikkelsen M, Jorgensen M, Krebs FC. The teraton challenge. A review of fixation and transformation of carbon dioxide. *Energy Environ. Sci.* 2010;3:43-81.
12. Snoeckx R, Aerts R, Tu X, Bogaerts A. Plasma-based dry reforming: A computational study ranging from the nanoseconds to seconds time scale. *J. Phys. Chem. C.* 2013;117:4957-4970.
13. Dorai R, Hassouni H, Kushner MJ. Interaction between soot particles and NOx during dielectric barrier discharge plasma remediation of simulated diesel exhaust. *J. Appl. Phys.* 2000;88:6060-6071.
14. Tao X, Bai M, Li X, Long H, Shaung S, Yin Y, Dai X. CH<sub>4</sub>-CO<sub>2</sub> reforming by plasma – challenges and opportunities. *Prog. Energy Combust. Sci.* 2011;37:113-124.
15. Xu C, Tu X. Plasma-assisted methane conversion in an atmospheric pressure dielectric barrier discharge reactor. *J. Energy Chem.* 2013;22:420-425.
16. Arts R, Somers W, Bogaerts A. Carbon dioxide splitting in a dielectric barrier discharge plasma: A combined experimental and computational study. *Chem Sus Chem.* 2015;8:702-716.
17. Kano M, Satoh G, Iizuka S. Reforming of carbon dioxide to methane and methanol by electric impulse low-pressure discharge with hydrogen. *Plasma Chem. Plasma Process.* 2012;32:177-185.
18. Tsuchiya T, Iizuka S. Conversion of methane to methanol by a low-pressure steam plasma. *J. Environ. Eng. Technol.* 2013;2:35-39.
19. Arita K, Iizuka S. Production of CH<sub>4</sub> in a low-pressure CO<sub>2</sub>/H<sub>2</sub> discharge with magnetic field. *J. Mater. Sci. Chem. Eng.* 2015;3:69-77.
20. Mazloomi K, Sulaiman N, Moayedi H. Electrical efficiency of electrolytic hydrogen production. *Int. J. Electrochem. Sci.* 2012;7:3314-3326.
21. Wei ZD, Ji MB, Chen SG, Liu Y, Sun CX, Yin GZ, Shen PK, Chan SH. Water electrolysis on carbon electrodes enhanced by surfactant. *Electrochem. Acta.* 2007;52:3323-3329.
22. Fujita S, Teruuma H, Nakamura M, Takezawa N. Mechanisms of methanation of carbon monoxide and carbon dioxide over nickel. *Ind. Eng. Chem. Res.* 1991;30:1146-1151.
23. Hoekman SK, Broch A, Robbins C, Purcell R. CO<sub>2</sub> recycling by reaction with renewably-generated hydrogen. *Int. J. Greenhouse Gas Contr.* 2010;4:44-50.

© 2016 Arita and Iizuka; This is an Open Access article distributed under the terms of the Creative Commons Attribution License (<http://creativecommons.org/licenses/by/4.0>), which permits unrestricted use, distribution, and reproduction in any medium, provided the original work is properly cited.

Peer-review history:

The peer review history for this paper can be accessed here:  
<http://sciencedomain.org/review-history/14425>